

Synthesis and Solid-State Polymerization of 5-(Pyren-1-yl)penta-2,4-diyne-1-ol Derivatives with an *N*-Phenylurethane or *N*-Benzylurethane Group

Shuhei Oshimizu, Shoko Takeshi, Tsubasa Sato, Ryohei Yamakado, Yoko Tatewaki, and Shuji Okada\*

Cite This: <https://dx.doi.org/10.1021/acs.cgd.0c00438>

Read Online

ACCESS |



Metrics &amp; More

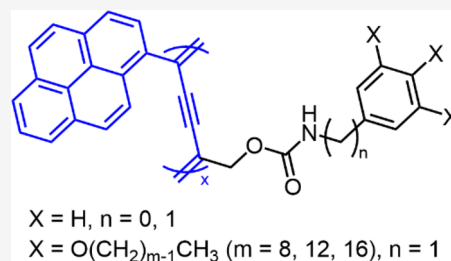


Article Recommendations



Supporting Information

**ABSTRACT:** A series of 5-(pyren-1-yl)penta-2,4-diyne-1-yl *N*-phenylcarbamates and *N*-benzylcarbamates were synthesized. Phenyl groups in the *N*-phenyl and *N*-benzyl moieties were unsubstituted (**H-0** and **H-1**, respectively) and 3,4,5-trialkoxy substituted (**C<sub>m</sub>O-0** and **C<sub>m</sub>O-1**, respectively), in which the alkyl groups introduced were methyl ( $m = 1$ ), octyl ( $m = 8$ ), dodecyl ( $m = 12$ ), and hexadecyl ( $m = 16$ ) groups. Upon UV irradiation, a regular 1,4-addition polymerization to form polydiacetylene was confirmed for **H-0**, **H-1**, **C<sub>8</sub>O-1**, **C<sub>12</sub>O-1**, and **C<sub>16</sub>O-1**. For **C<sub>1</sub>O-0** and **C<sub>1</sub>O-1**, the crystal structures were solved, and the reasons the regular polymerization did not occur were clarified. From the powder X-ray diffraction study, crystallinities of **C<sub>m</sub>O-1** were found to be lower than those of **C<sub>m</sub>O-0**, although **C<sub>m</sub>O-1** regularly polymerized. This indicates that the total crystallinity is not directly related to local ordering around one-dimensional arrays for the polymerization direction. Polymerized **C<sub>m</sub>O-1** species were soluble in chloroform. Their processability enabled us to fabricate cast films of polydiacetylene as well as the monomer. The conductivities of **C<sub>12</sub>O-1** and the polymer (**PC<sub>12</sub>O-1**) were evaluated in the pristine and iodine-doped states and in the charge-transfer-complexed states with 2,3,5,6-tetrafluoro-7,7,8,8-tetracyanoquinodimethane. A conductivity of  $1.2 \times 10^{-2} \text{ S m}^{-1}$  for iodine-doped **PC<sub>12</sub>O-1** was achieved. In this case, pyrene moieties seemed to play an important role in realizing the appropriate electron transfer from pyrene moieties to iodine molecules and effective  $\pi$  conjugation between the pyrene moieties and the PDA backbone promoting charge transport.



## INTRODUCTION

A variety of  $\pi$ -conjugated polymers have been investigated as materials for nonlinear optics,<sup>1–3</sup> electric conduction,<sup>4–6</sup> electrochromism,<sup>7–9</sup> light emission,<sup>10–12</sup> photovoltaics,<sup>13–16</sup> transistors,<sup>17–19</sup> sensors,<sup>20–22</sup> etc., and many of them have generally been synthesized via solution polymerization. However, polydiacetylene (PDA) is an exception. It is synthesized by the solid-state 1,4-addition polymerization of butadiyne monomers.<sup>23</sup> Since polymerization progresses topochemically, the resulting polymers can have quite regular stereostructures with high molecular weight. Although this is a kind of ideal polymerization, it also has challenges. First, the butadiyne monomers synthesized do not polymerize with a high probability because of narrow acceptable conditions for the solid-state polymerization. The monomers should satisfy the following conditions to react via regular 1,4-addition polymerization: the distance  $d$  between the adjacent monomers in the array with the translation relation is approximately 0.5 nm and angle  $\theta$  between the translation axis and the butadiyne rod in the monomer is approximately  $45^\circ$ , as shown in Figure 1.<sup>24,25</sup> Second, the polymers obtained are generally insoluble and the processability is poor. However, since PDA has a  $\pi$ -conjugated backbone, a wide range of electronic and optical applications have been considered in general. Thus, the molecular design and the related properties

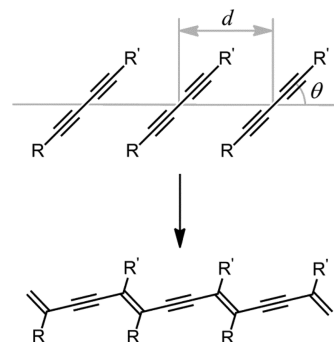


**Figure 1.** Topochemical polymerization scheme of butadiyne derivatives. Appropriate conditions for the regular 1,4-addition polymerization are a distance  $d$  of approximately 0.5 nm and an angle  $\theta$  of approximately  $45^\circ$ .

Received: March 31, 2020

Revised: August 4, 2020

Published: August 5, 2020

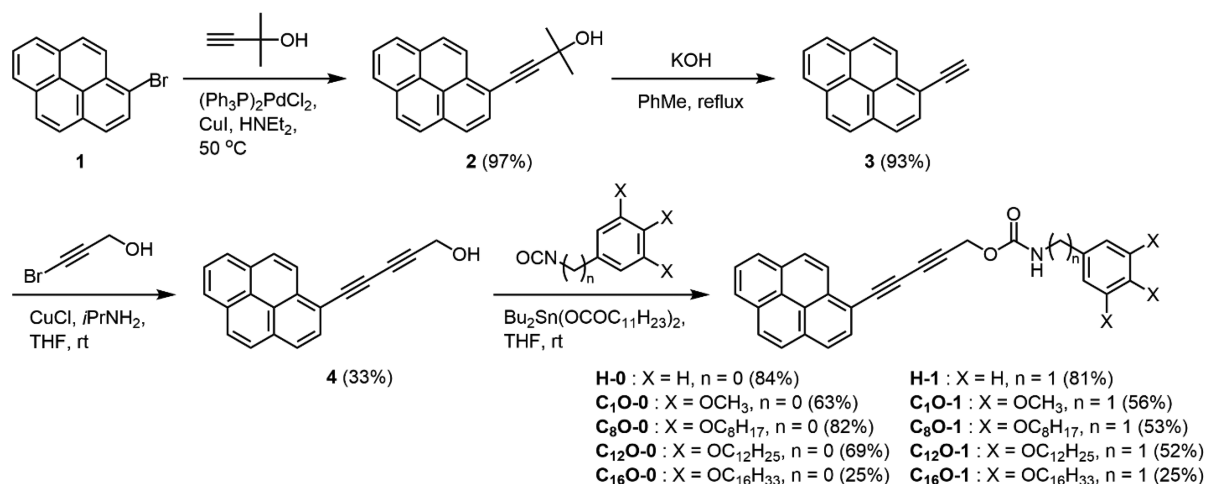


**Figure 2.** Synthesis scheme of pyrenylbutadiyne derivatives with an *N*-phenylurethane or *N*-benzylurethane moiety.

have been extensively investigated. The properties investigated are, for example, third-order nonlinear optical properties,<sup>1,26–31</sup> conductivities,<sup>32–37</sup> colorimetric properties,<sup>38–41</sup> etc.

From the viewpoint of the molecular design of PDA, PDAs with  $\pi$  conjugation between the backbone and substituents are interesting because of their improved electronic and optical properties.<sup>42</sup> However, the probability of solid-state polymerization of butadiyne monomers directly substituted by aromatic rings is lower than that of the monomers substituted by alkyl groups in general. Thus, strategies to align the monomers in polymerizable stacks are required. One of the strategies is to use a supramolecular host–guest system.<sup>43,44</sup> The other is modification by specific groups, which tend to align monomers in one-dimensional (1D) arrays. We have used the latter strategy to prepare butadiyne monomers with  $\pi$  conjugation between the backbone and substituents.<sup>45,46</sup> For example, butadiyne derivatives directly bound to electron-donating aromatics such as pyrene,<sup>47,48</sup> *N*-phenylcarbazole,<sup>49,50</sup> aniline,<sup>51,52</sup> and tetrathiafluvalene (TTF)<sup>53</sup> were recently synthesized, and some of them polymerized regularly to form PDAs with conjugated donors. Meanwhile, in order to improve the PDA processability, one of the potential approaches is its solubilization. Although some butadiyne derivatives with urethane groups have been found to dissolve in organic solvent,<sup>54,55</sup> we prepared those with 3,4,5-trialkoxyphenyl (TAOP) groups to impart self-organizing properties and solubilities of their polymers.<sup>56,57</sup>

In the present study, we focused on the preparation of soluble PDAs with donor substituents directly bound to the  $\pi$ -conjugated backbone. As a donor, we selected pyrene because of its relatively high photostability, and TAOP groups were introduced for solubilization. The alkyl chains in the TAOP groups were varied among octyloxy, dodecyloxy, and hexadecyloxy groups. For comparison, the derivatives with a simple phenyl group instead of the TAOP group or with the TAOP group containing methoxy groups were also synthesized. The photopolymerizability and crystallinity of the monomers and processability of the polymers were investigated. The electrical conductivities of the films of a monomer and the corresponding polymer were evaluated.

## RESULTS AND DISCUSSION

Ten pyrenylbutadiyne derivatives with an *N*-phenylurethane or *N*-benzylurethane moiety were synthesized according to Figure 2. From 1-bromopyrene (**1**), 1-ethynylpyrene (**3**) was prepared via **2** as a product of Sonogashira coupling followed by acetone elimination using potassium hydroxide. A Cadiot–Chodkiewicz coupling reaction between **3** and 3-bromoprop-2-yn-1-ol afforded 5-(pyren-1-yl)penta-2,4-diyne-1-ol (**4**). Finally, addition reaction of isocyanates to **4** gave the desired compounds.

First, photopolymerization behaviors of the solid samples were investigated using visible diffuse reflectance spectra (see the Experimental Section for the sample preparation). Figure 3 shows the spectra obtained by UV irradiation of 254 nm. All pyrenylbutadiyne derivatives showed an absorption increase in the visible region, suggesting that polymerization occurred to form extended  $\pi$ -conjugated structures. The spectral patterns are roughly classified into two categories. Compounds in the first category (type I) showed spectra having absorption maxima in the wavelength range between 550 and 700 nm after UV irradiation. Compounds of type I are **H-0**, **H-1**, **C<sub>8</sub>O-1**, **C<sub>12</sub>O-1**, and **C<sub>16</sub>O-1**, whose absorption maxima at the longest wavelengths were 646, 691, 668, 659, and 667 nm, respectively. These absorption bands are generally assigned to an excitonic absorption with its phonon sidebands originating from the regularly polymerized PDA structure. Other compounds in the second category (type II) showed an absorption increase in the visible region upon UV irradiation but no absorption maxima were observed in this region. In this case, the polymerization scheme seems to be not as regular as for the compounds of type I. Actually, in our previous study, we confirmed by single-crystal X-ray crystallographic analysis that the butadiyne derivatives showing the polymer absorption of type II aligned under the conditions with a large deviation from  $d = 0.5$  nm and  $\theta = 45^\circ$  in Figure 1.<sup>52</sup>

Powder X-ray diffraction patterns of the monomers were obtained as shown in Figure 4. Sharp diffraction peaks were observed for the compounds with phenyl or trimethoxyphenyl groups: i.e., **H-0**, **H-1**, **C<sub>1</sub>O-0**, and **C<sub>1</sub>O-1**. Among these compounds, single crystals of **C<sub>1</sub>O-0** and **C<sub>1</sub>O-1** with large enough sizes for X-ray crystallography were obtained and analyzed. The crystal structures of **C<sub>1</sub>O-0** and **C<sub>1</sub>O-1** are shown in Figures 5 and 6, respectively, and their crystallographic data are summarized in Table 1. **C<sub>1</sub>O-0** molecules

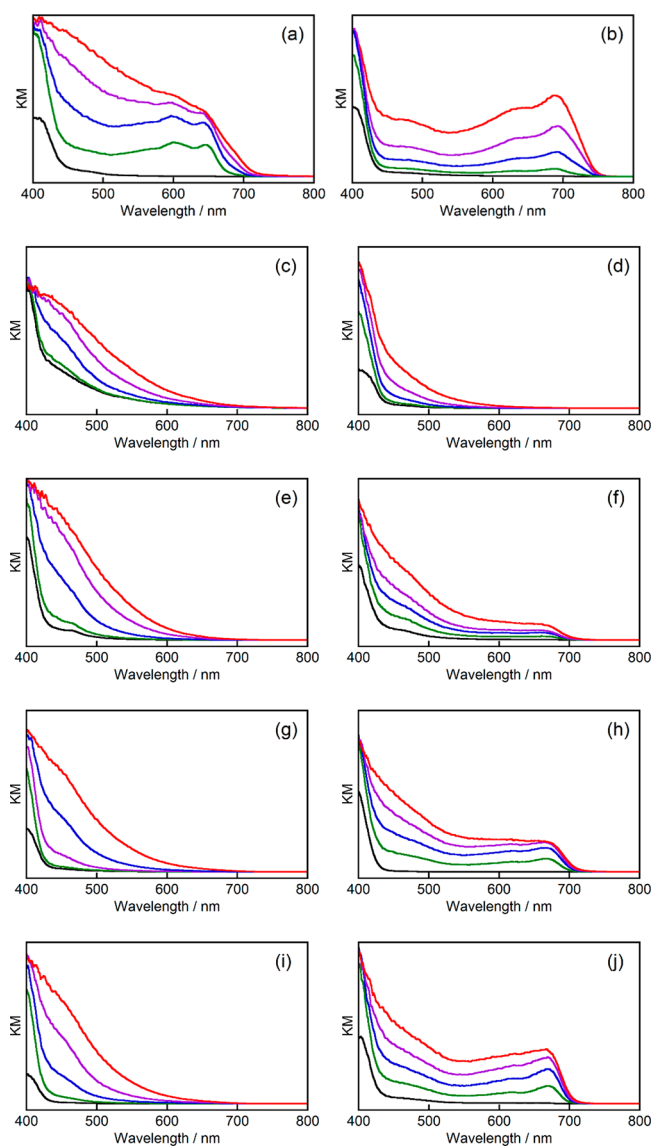


**Figure 3.** Visible diffuse reflectance spectra of (a) H-0, (b) H-1, (c) C<sub>1</sub>O-0, (d) C<sub>1</sub>O-1, (e) C<sub>8</sub>O-0, (f) C<sub>8</sub>O-1, (g) C<sub>12</sub>O-0, (h) C<sub>12</sub>O-1, (i) C<sub>16</sub>O-0, and (j) C<sub>16</sub>O-1 in the course of UV irradiation at 254 nm. Black, green, blue, violet, and red lines correspond to the spectra after UV irradiation for 0, 5, 30, 120, and 480 min, respectively.

form 1D stacking along the *b* axis due to the intermolecular hydrogen bonding between urethane groups (green dashed lines in Figure 5b). The distance *d* and angle  $\theta$ , defined in Figure 1, are 0.476 nm and 65.6°, respectively. In comparison with the polymerizable conditions, *d* is slightly shorter and  $\theta$  is larger. The carbon–carbon (C–C) distances between adjacent molecules are 0.438, 0.443, and 0.470 nm for C1–C2, C3–C4, and C1–C4, respectively, whose carbon numbers are indicated in Figure 5b. Namely, C–C distances for 1,2-addition (C1–C2 and C3–C4) are shorter than those of 1,4-addition (C1–C4). This result is clear evidence that C<sub>1</sub>O-0 does not polymerize in the regular 1,4-addition manner, resulting in absorption spectra of C<sub>1</sub>O-0 without an excitonic peak after UV irradiation (Figure 3c). Unexpectedly for C<sub>1</sub>O-1, there are no hydrogen bonds between urethane groups but the nitrogen atom of the urethane group forms an intermolecular hydrogen bond with the oxygen atom of a methoxy group (green dashed lines in Figure 6a). As a result, the carboxy group in the urethane bond

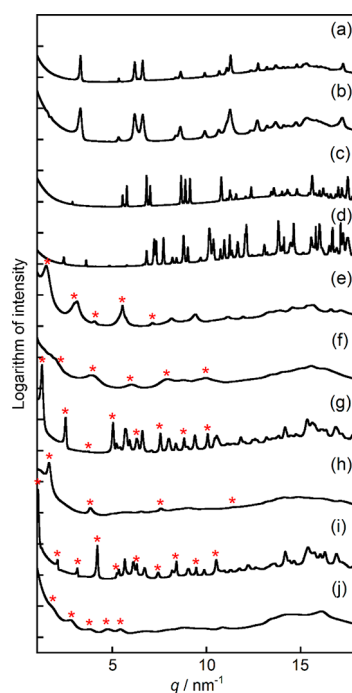


**Figure 4.** Powder X-ray diffraction patterns of (a) H-0, (b) H-1, (c) C<sub>1</sub>O-0, (d) C<sub>1</sub>O-1, (e) C<sub>8</sub>O-0, (f) C<sub>8</sub>O-1, (g) C<sub>12</sub>O-0, (h) C<sub>12</sub>O-1, (i) C<sub>16</sub>O-0, and (j) C<sub>16</sub>O-1. One scale of the vertical axis corresponds to 1 (=log 10), and the lowermost scale is 2 (=log 10<sup>2</sup>) for each curve, which is shifted by 2 to avoid overlap. Red asterisks on the peak tops of the diffractograms (e)–(j) indicate that these peaks were used to calculate the interlayer spacings.

of C<sub>1</sub>O-1 does not form a hydrogen bond. This fact is also supported by the IR spectral data. Almost all urethane compounds in this study showed an absorption peak corresponding to a C=O stretching vibration in the range of 1693–1697 cm<sup>-1</sup>, suggesting intermolecular hydrogen bonding of the urethane groups. However, C<sub>1</sub>O-1 exceptionally exhibited the peak at a higher wavenumber of 1722 cm<sup>-1</sup>, indicating an isolated C=O bond without hydrogen bonding. As shown in Figure 6b, pyrene and butadiyne moieties of C<sub>1</sub>O-1 are alternately piled up. Thus, a regular 1,4-addition polymerization is impossible in this crystal. Among the powder X-ray diffractograms of the compounds with other trialkoxyphenyl groups, C<sub>12</sub>O-0 and C<sub>16</sub>O-0 showed clear progression of the peaks related to the layered structures, and the interlayer spacings were calculated to be 5.00 and 5.99 nm, respectively. In comparison with these, C<sub>8</sub>O-0 showed weaker and broad peaks, and the spacing was roughly estimated to be 4.4 nm. Namely, longer alkyl chains of the compound tend to give a larger spacing. C<sub>8</sub>O-1, C<sub>12</sub>O-1, and C<sub>16</sub>O-1 showed much weaker diffraction peaks, suggesting their lower crystallinity. However, C<sub>12</sub>O-1 showed a progression of the peaks corresponding to a spacing of about 3.3 nm. Although the peaks of C<sub>8</sub>O-1 and C<sub>16</sub>O-1 were broad, the spacings were roughly estimated to be 3.2 and 6.8 nm, respectively. The relationship between the alkyl chain length and the spacing of C<sub>*m*</sub>O-1 is similar to that of C<sub>*m*</sub>O-0. However, the spacing of C<sub>16</sub>O-1 is slightly more than twice the spacing of C<sub>8</sub>O-1 or C<sub>12</sub>O-1. This may suggest that the periodic structure of C<sub>16</sub>O-1 is the bilayer type but that of C<sub>8</sub>O-1 or C<sub>12</sub>O-1 is the monolayer type. The melting points of C<sub>*m*</sub>O-0 are higher than those of the corresponding C<sub>*m*</sub>O-1, respectively, and these

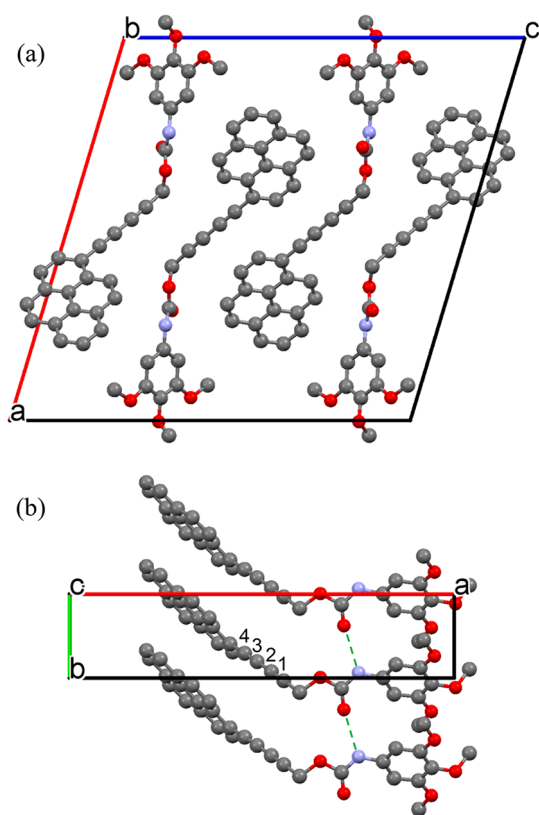


**Figure 5.** Crystal structure of  $C_1O-0$  viewed along (a) the  $b$  axis and (b) the  $c$  axis. Green dashed lines in (b) indicate intermolecular hydrogen bonds. Numbers labeling  $sp$  carbons in (b) are to enable an explanation of the carbon–carbon distance in the text. Atom color code: gray, blue, and red refer to carbon, nitrogen, and oxygen, respectively.

differences may originate from the crystallinity. As described above,  $C_mO-1$  with less crystallinity regularly polymerized and  $C_mO-0$  with more crystallinity did not. This fact seems contradictory. However, a similar situation, i.e., polymerizable butadiyne moieties in a less crystalline environment, can be found in segmented copolymers composed of polyurethane or polyamide with butadiyne moieties in the backbone.<sup>58–60</sup> In these polymers, the butadiyne moieties stacked regularly in the hard segment, which are surrounded by the amorphous soft segment, can polymerize in the 1,4-addition manner. In the less crystalline  $C_mO-1$ , the butadiyne moieties are properly aligned but the methylene group in the benzyl urethane moiety may prevent an ordered assembling of the alkyl chains of TAOP groups. The contrast in crystallinity between  $C_mO-0$  and  $C_mO-1$  are interesting, although the more detailed structural differences were not able to be clarified. Regardless of polymerization in the regular manner or not, a close contact of the pyrene moieties was confirmed in the solid state of this series of compounds because a broad emission attributed to pyrene excimer formation was observed in the fluorescence spectra in the solid state (Figure S1).

$C_{12}O-1$  after UV irradiation for 12 h was dissolved in chloroform, and the solution was added dropwise in methanol to reprecipitate. The yields of the polymer precipitated were 10–15%. The UV–vis spectrum of the resulting precipitate portion ( $PC_{12}O-1$ ) dissolved in chloroform is shown in Figure 7. The absorption maximum at 612 nm of the PDA structure was clearly observed even in chloroform, although the

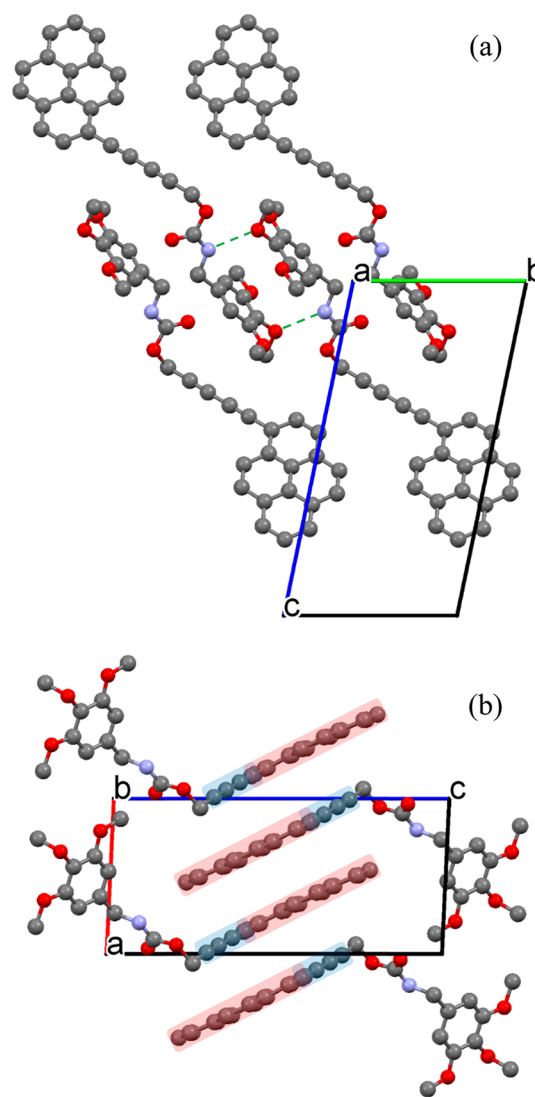


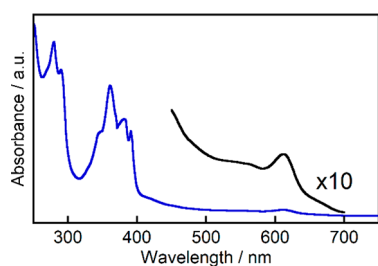
**Figure 6.** Crystal structure of  $C_1O-1$  viewed along (a) the  $a$  axis and (b) the  $b$  axis. Green dashed lines in (a) indicate intermolecular hydrogen bonds. In (b), red and blue rectangles indicate pyrene and butadiyne moieties, respectively. Atom color code: gray, blue, and red refer to carbon, nitrogen, and oxygen, respectively.

absorption maximum wavelength has been blue-shifted from that in the crystalline state at 659 nm. This blue shift may be due to less planarity of the  $\pi$ -conjugated backbone with the solvated side chains. Photopolymerized  $C_8O-1$  and  $C_{16}O-1$  were also soluble in chloroform. The chloroform solution of the polymerized sample of  $C_{12}O-1$  with 1 g L<sup>-1</sup> concentration, which was filtered by a membrane filter with a pore size of 0.45  $\mu$ m, was subjected to GPC, and the elution curve in Figure 8 was obtained. The molecular weight distribution was quite broad from the oligomer level to polymers with a molecular weight of more than  $1 \times 10^6$ , which is about the exclusion limit of the columns. A dip in the elution curve at a retention time of about 35 min corresponded to a molecular weight of about  $6 \times 10^3$  of the standard polystyrene. If the components are divided at this molecular weight, the higher-molecular-weight components accounted for about 60% of the product, which is simply estimated by the area of the elution curve.

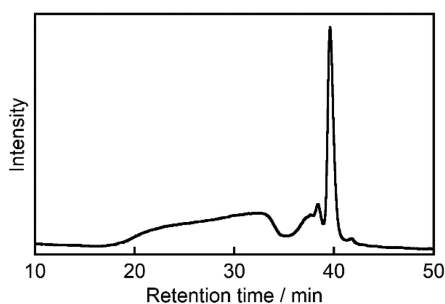
In order to investigate the function of the pyrenyl group introduced, experiments on chemical doping were performed.

Table 1. Crystallographic Data of C<sub>12</sub>O-0 and C<sub>12</sub>O-1

	C <sub>12</sub> O-0	C <sub>12</sub> O-1
formula	C <sub>31</sub> H <sub>23</sub> NO <sub>5</sub>	C <sub>32</sub> H <sub>23</sub> NO <sub>5</sub>
formula wt	489.50	503.53
cryst syst	monoclinic	triclinic
space group	<i>P</i> 2 <sub>1</sub> / <i>c</i>	<i>P</i> $\bar{1}$
<i>a</i> /Å	22.7495(13)	8.030(13)
<i>b</i> /Å	4.7604(3)	8.963(16)
<i>c</i> /Å	22.7650(13)	17.65(4)
$\alpha$ /deg	90	101.61(8)
$\beta$ /deg	106.637(4)	92.09(6)
$\gamma$ /deg	90	92.97(6)
<i>V</i> /Å <sup>3</sup>	2362.2(2)	1241(4)
<i>Z</i>	4	2
<i>D<sub>x</sub></i> /Mg m <sup>-3</sup>	1.376	1.347
<i>R</i>	0.0483	0.0669
<i>R<sub>w</sub></i>	0.1102	0.1470
GOF	1.057	0.988
<i>T</i> /K	90(2)	100(2)



**Figure 7.** UV-vis absorption spectrum of the chloroform solution of PC<sub>12</sub>O-1 (blue curve). A magnified spectrum is shown between 450 and 750 nm using a black curve. The solution measured was prepared as follows: C<sub>12</sub>O-1 after irradiation of UV at 254 nm for 12 h was dissolved in chloroform, and the resulting solution was filtered by a membrane filter with a pore size of 0.45 μm.



**Figure 8.** GPC elution curve of polymerized C<sub>12</sub>O-1.

By using C<sub>12</sub>O-1 as a base compound, the four film samples, which were generally amorphous, were prepared on glass slides with gold electrodes, and their DC electrical conductivities were evaluated by the two-probe method (Table 2). Sample 1a was prepared by casting a C<sub>12</sub>O-1 chloroform solution. Iodine vapor treatment of sample 1a gave sample 1b, and sample 1c was obtained by keeping sample 1b in air for a prolonged time to remove iodine. Similar samples 3a–c were prepared for the corresponding PDA of PC<sub>12</sub>O-1. Before iodine treatment and after removal of iodine, the conductivities of C<sub>12</sub>O-1 and PC<sub>12</sub>O-1 at room temperature were on the order of 10<sup>-8</sup>–10<sup>-7</sup> S m<sup>-1</sup>. Since the conductivities of pristine PDAs are reported to be on the order of 10<sup>-14</sup>–10<sup>-7</sup> S m<sup>-1</sup>,<sup>61–67</sup> those of C<sub>12</sub>O-1

Table 2. Electric Conductivities ( $\sigma$ ) of C<sub>12</sub>O-1, PC<sub>12</sub>O-1, and Their Charge-Transfer States

sample	donor	acceptor	$\sigma$ /S m <sup>-1</sup>	remark
1a	C <sub>12</sub> O-1		2.3 × 10 <sup>-7</sup>	pristine
1b		I <sub>2</sub>	8.4 × 10 <sup>-5</sup>	I <sub>2</sub> vapor treatment of sample 1a
1c			1.7 × 10 <sup>-7</sup>	sample 1b kept in air to remove I <sub>2</sub>
2	C <sub>12</sub> O-1	F <sub>4</sub> TCNQ	1.4 × 10 <sup>-5</sup>	1:1 molar ratio
3a	PC <sub>12</sub> O-1		1.9 × 10 <sup>-8</sup>	pristine
3b		I <sub>2</sub>	1.2 × 10 <sup>-2</sup>	I <sub>2</sub> vapor treatment of sample 3a
3c			5.0 × 10 <sup>-8</sup>	sample 3b kept in air to remove I <sub>2</sub>
4	PC <sub>12</sub> O-1	F <sub>4</sub> TCNQ	1.3 × 10 <sup>-4</sup>	1:1 molar ratio

and PC<sub>12</sub>O-1 are within the range but are relatively high. During iodine doping, the conductivities of C<sub>12</sub>O-1 and PC<sub>12</sub>O-1 increased, and they were finally saturated at 8.4 × 10<sup>-5</sup> and 1.2 × 10<sup>-2</sup> S m<sup>-1</sup>, respectively. Due to the conjugated backbone of PC<sub>12</sub>O-1, about a 2 orders of magnitude conductivity enhancement was confirmed, in comparison with C<sub>12</sub>O-1. Since pyrene is an electron donor and charge-transfer (CT) complexes of pyrene and 7,7,8,8-tetracyanoquinodimethane (TCNQ) derivatives have been known,<sup>68–73</sup> we prepared CT complexes of C<sub>12</sub>O-1 and PC<sub>12</sub>O-1 with 2,3,5,6-tetrafluoro-7,7,8,8-tetracyanoquinodimethane (F<sub>4</sub>TCNQ). For the CT complex preparation, chloroform solutions of C<sub>12</sub>O-1 or PC<sub>12</sub>O-1 were mixed with F<sub>4</sub>TCNQ acetone solution in a 1:1 molar ratio and the solvents were evaporated. Figure 9

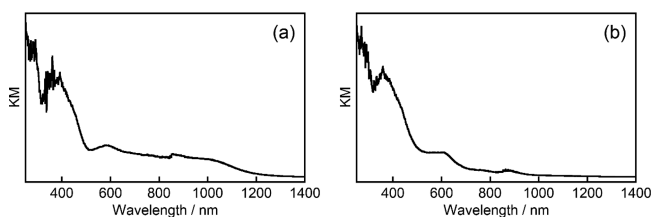


**Figure 9.** UV-vis-NIR diffuse reflectance spectra of CT complexes with F<sub>4</sub>TCNQ: (a) C<sub>12</sub>O-1/F<sub>4</sub>TCNQ; (b) PC<sub>12</sub>O-1/F<sub>4</sub>TCNQ. The molar ratio of F<sub>4</sub>TCNQ with respect to C<sub>12</sub>O-1 and the PC<sub>12</sub>O-1 monomer unit was 1:1.

shows UV-vis-NIR diffuse reflectance spectra of the complexes C<sub>12</sub>O-1/F<sub>4</sub>TCNQ and PC<sub>12</sub>O-1/F<sub>4</sub>TCNQ. In the spectrum of C<sub>12</sub>O-1/F<sub>4</sub>TCNQ, a broad CT band from around 1200 nm to the visible region was observed. Although C<sub>12</sub>O-1/F<sub>4</sub>TCNQ was irradiated at a UV wavelength of 254 nm, apparent spectral changes were not detected, indicating that the complex is photostable and not polymerizable. The spectrum of PC<sub>12</sub>O-1/F<sub>4</sub>TCNQ also showed a broad CT band from the NIR to visible region, but it seemed to be weaker than that of C<sub>12</sub>O-1/F<sub>4</sub>TCNQ. Since the peak at approximately 600 nm remained, the PDA backbone structure was considered to be maintained. The conductivities of C<sub>12</sub>O-1/F<sub>4</sub>TCNQ and PC<sub>12</sub>O-1/F<sub>4</sub>TCNQ were evaluated to be 1.4 × 10<sup>-5</sup> and 1.3 × 10<sup>-4</sup> S m<sup>-1</sup>, respectively. When the conductivities were compared between iodine-doped and CT-complexed samples, higher conductivities were obtained for the former samples of both the monomer and polymer,

indicating that better CT states for electric conduction were achieved in iodine doping in these cases. For the iodine-doped PDAs in general, the conductivities have been reported to be on the order of  $10^{-8}$ – $10^{-4}$  S  $m^{-1}$ .<sup>32–37,62</sup> By using other dopants and polymerization under high pressure, the conductivities of PDA increased up to  $10^{-3}$  S  $m^{-1}$ .<sup>74</sup> In the present study, the conductivity of the iodine-doped PC<sub>12</sub>O-1 was measured to be as high as  $10^{-2}$  S  $m^{-1}$ , which may be due to an appropriate charge transfer from the pyrene moieties to iodine molecules and effective  $\pi$  conjugation between the pyrene moieties and the PDA backbone.

## CONCLUSION

Ten pyrenyl-substituted PDAs with a urethane moiety were prepared. Regular 1,4-addition polymerization was confirmed for H-0, H-1, C<sub>8</sub>O-1, C<sub>12</sub>O-1, and C<sub>16</sub>O-1, which showed characteristic excitonic absorption peaks between 646 and 691 nm. Although C<sub>1</sub>O-0 and C<sub>1</sub>O-1 were not polymerized in the regular manner, the crystal structures were able to be analyzed and the reasons they did not regularly polymerize were clarified. For C<sub>1</sub>O-0, 1D monomer arrays due to the intermolecular hydrogen bonding between urethane groups were formed. However,  $d$  was shorter and  $\theta$  was larger with respect to the regularly polymerizable conditions. For C<sub>1</sub>O-1, intermolecular hydrogen bonding was not formed between urethane groups but formed between urethane and methoxy groups, which resulted in alternating stacking of pyrene and butadiyne moieties. Although the introduction of a urethane or amide group in butadiyne monomers promotes the formation of 1D arrays in the crystals in general, this principle is sometimes broken. For longer alkyl derivatives, crystallinities of C<sub>*m*</sub>O-1 were lower than those of C<sub>*m*</sub>O-0 despite the regular polymerization of C<sub>*m*</sub>O-1. This fact indicates that local ordering around 1D arrays for the polymerization direction may not be reflected in the total crystallinity. Polymerized C<sub>*m*</sub>O-1 is soluble in chloroform and processable. Solution-cast films of C<sub>12</sub>O-1, PC<sub>12</sub>O-1, and their CT complexes with F<sub>4</sub>TCNQ were prepared. For the C<sub>12</sub>O-1 and PC<sub>12</sub>O-1 films, iodine doping was performed and their conductivities were evaluated. The highest conductivity among the measured conditions was  $1.2 \times 10^{-2}$  S  $m^{-1}$  for iodine-doped PC<sub>12</sub>O-1, in which appropriate charge transfer and effective  $\pi$  conjugation between the substituents and the PDA backbone seemed to be achieved.

## EXPERIMENTAL SECTION

**Materials.** Commercially available reagents and solvents were used as received except for copper(I) chloride, which was washed with hydrochloric acid (2 mol/L) and vacuum-dried in an oven at 100 °C. The synthesis procedures of alkoxy-substituted phenyl isocyanates<sup>55</sup> 9a–d and benzyl isocyanates 15a–d are described in the Supporting Information.

**2-Methyl-4-(pyren-1-yl)but-3-yn-2-ol (2).** A mixture of 1-bromopyrene (1; 5.00 g, 17.8 mmol) and bis(triphenylphosphine)-palladium(II) dichloride (0.19 g, 0.27 mmol) in diethylamine (26 mL) was stirred at 50 °C until all compounds were dissolved. Then, 2-methyl-3-butyn-2-ol (1.85 mL, 18.9 mmol) and copper(I) iodide (51.4 mg, 0.27 mmol) were added, and the mixture was refluxed overnight. After the solvent was removed from the reaction mixture, chloroform was added and washed with water. The organic layer was dried over anhydrous sodium sulfate, and the solvent in the filtrate was removed under reduced pressure. The residue was purified by column chromatography (silica gel, chloroform/ethyl acetate 9/1) to afford 2 (4.90 g, 17.2 mmol, 97%) as a dark orange solid: mp 116 °C;

IR (KBr) 3305, 3035, 2978, 2931, 1162, 964, 845, 715  $cm^{-1}$ ; <sup>1</sup>H NMR (400 MHz, CDCl<sub>3</sub>)  $\delta$  1.79 (6H, s), 2.77 (1H, br s), 7.80–8.03 (8H, m), 8.46 (1H, d,  $J$  = 8.8 Hz); <sup>13</sup>C NMR (100 MHz, CDCl<sub>3</sub>)  $\delta$  31.67, 65.94, 81.15, 99.35, 116.93, 123.96, 124.08, 124.17, 125.07, 125.31, 125.36, 125.94, 126.93, 127.85, 128.07, 129.39, 130.73, 130.92, 130.95, 131.66.

**1-Ethynylpyrene (3).** A mixture of 2 (4.90 g, 17.2 mmol) and mashed potassium hydroxide (0.981g, 17.5 mmol) in toluene (100 mL) was refluxed for 30 min. After filtration, the solvent in the filtrate was removed under reduced pressure. The residue was purified by column chromatography (silica gel, chloroform) to afford 3 (3.62 g, 16.0 mmol, 93%) as a brown solid: mp 115 °C; IR (KBr) 3296, 3033, 2094, 1600, 839, 714, 644, 593  $cm^{-1}$ ; <sup>1</sup>H NMR (400 MHz, CDCl<sub>3</sub>)  $\delta$  3.56 (1H, s), 7.82–8.06 (8H, m), 8.46 (1H, d,  $J$  = 9.2 Hz); <sup>13</sup>C NMR (100 MHz, CDCl<sub>3</sub>)  $\delta$  82.45, 82.75, 116.28, 123.93, 124.08, 124.19, 125.08, 125.49, 125.55, 126.06, 126.94, 128.18, 128.35, 129.96, 130.74, 130.93, 131.36, 132.29.

**5-(Pyren-1-yl)penta-2,4-diyne-1-ol (4).** A mixture of copper(I) chloride (43.8 mg, 0.442 mmol) and a spatulafull of hydroxylammonium chloride in isopropylamine (30 mL) was stirred under a nitrogen atmosphere. To this were added 3-bromoprop-2-yn-1-ol (2.20 g 16.3 mmol) and 3 (2.00 g 8.84 mmol) in 28 mL of anhydrous tetrahydrofuran (THF) dropwise for 30 min. When the mixture became dark during the addition, a small amount of hydroxylammonium chloride was added until the mixture turned yellow. This mixture was further stirred overnight. After the solvent in the reaction mixture was removed, chloroform was added and this solution was washed with water. The organic layer was dried over anhydrous sodium sulfate. After filtration, the solvent in the filtrate was removed under reduced pressure. The residue was purified by column chromatography (silica gel, chloroform/ethyl acetate 9/1) and recrystallized from a mixture of chloroform and hexane to afford 4 (0.82 g, 2.93 mmol, 33%) as a pale orange powder: mp 123 °C dec; IR (KBr) 3367, 3035, 2917, 2852, 2227, 1600, 1596, 1392, 1007, 839, 713  $cm^{-1}$ ; <sup>1</sup>H NMR (400 MHz, CDCl<sub>3</sub>)  $\delta$  1.92 (1H, br s), 4.52 (2H, s), 7.94–8.18 (8H, m), 8.47 (1H, d,  $J$  = 9.2 Hz); <sup>13</sup>C NMR (100 MHz, CDCl<sub>3</sub>)  $\delta$  51.83, 70.86, 78.06, 78.41, 81.84, 115.42, 123.93, 124.14, 124.40, 125.03, 125.84, 125.90, 126.30, 127.03, 128.72, 128.81, 130.49, 130.80, 131.00, 131.83, 133.32.

**5-(Pyren-1-yl)penta-2,4-diyne-1-yl N-Phenylcarbamate (H-0).** A mixture of 4 (50.0 mg, 0.178 mmol), phenyl isocyanate (27.2 mg, 0.228 mmol), and a few drops of dibutyltin dilaurate in anhydrous THF (20 mL) was stirred overnight at ambient temperature. After the solvent was removed under reduced pressure, the residue was purified by column chromatography (silica gel, chloroform/ethyl acetate 9/1) and recrystallized from a mixture of chloroform and hexane to afford H-0 (60.0 mg, 0.150 mmol, 84%) as a pale yellow powder: mp 167 °C; IR (KBr) 3294, 3032, 2920, 2235, 1695, 1552, 1448, 1358, 1255, 1135, 1055, 978, 850, 754, 698  $cm^{-1}$ ; <sup>1</sup>H NMR (400 MHz, CDCl<sub>3</sub>)  $\delta$  5.03 (2H, s), 6.77 (1H, br s), 7.11 (1H, t,  $J$  = 7.2 Hz), 7.34 (2H, t,  $J$  = 7.2 Hz), 7.43 (2H, d,  $J$  = 7.2 Hz), 8.00–8.23 (8H, m), 8.51 (1H, d,  $J$  = 9.0 Hz); <sup>13</sup>C NMR (100 MHz, CDCl<sub>3</sub>)  $\delta$  53.54, 71.76, 77.72, 78.30, 78.40, 115.25, 118.76, 123.89, 124.00, 124.22, 124.42, 125.10, 125.95, 126.01, 126.40, 127.10, 128.88, 128.95, 129.14, 130.64, 130.87, 131.06, 132.01, 133.50, 137.31, 152.32. Anal. Found: C, 83.84; H, 4.07; N, 3.48. Calcd for C<sub>28</sub>H<sub>17</sub>NO<sub>2</sub>: C, 84.19; H, 4.29; N, 3.51.

**5-(Pyren-1-yl)penta-2,4-diyne-1-yl N-Benzylcarbamate (H-1).** A mixture of 4 (320 mg, 1.14 mmol), benzyl isocyanate (197 mg, 1.47 mmol), and a few drops of dibutyltin dilaurate in anhydrous THF (20 mL) was stirred overnight at ambient temperature. After the solvent was removed, the residue was purified by column chromatography (silica gel, chloroform/ethyl acetate 9/1) and recrystallized from a mixture of chloroform and hexane to afford H-1 (380 mg, 0.919 mmol, 81%) as an orange powder: mp 148 °C; IR (KBr) 3294, 3029, 2920, 2233, 1695, 1550, 1448, 1357, 1254, 1134, 1053, 976, 850, 756, 698  $cm^{-1}$ ; <sup>1</sup>H NMR (400 MHz, CDCl<sub>3</sub>)  $\delta$  4.41 (2H, d,  $J$  = 5.9 Hz), 4.95 (2H, s), 5.22 (1H, br s), 7.26–7.36 (5H, m), 7.92–8.17 (8H, m), 8.44 (1H, d,  $J$  = 9.1 Hz); <sup>13</sup>C NMR (100 MHz, CDCl<sub>3</sub>)  $\delta$  45.23, 53.39, 71.42, 78.17, 78.21, 78.39, 115.24, 123.88, 124.09, 124.32, 125.01, 125.84, 125.91, 126.29, 126.99, 127.52, 127.59, 128.70,

128.74, 128.82, 130.53, 130.77, 130.97, 131.87, 133.36, 137.97, 155.42. Anal. Found: C, 84.16; H, 4.42; N, 3.39. Calcd for  $C_{29}H_{19}NO_2$ : C, 84.24; H, 4.63; N, 3.39.

**5-(Pyren-1-yl)penta-2,4-diynyl N-(3,4,5-Trimethoxyphenyl)carbamate (C<sub>1</sub>O-0).** A mixture of **4** (100 mg, 0.357 mmol), crude 3,4,5-trimethoxyphenyl isocyanate (**9a**; 1.64 g), and a few drops of dibutyltin dilaurate in anhydrous THF (30 mL) was stirred overnight at ambient temperature. After the solvent in the reaction mixture was removed, the residue was purified by column chromatography (silica gel, chloroform/ethyl acetate 9/1) and recrystallized from a mixture of chloroform and methanol to afford **C<sub>1</sub>O-0** (110 mg, 0.225 mmol, 63%) as a pale orange powder: mp 193 °C; IR (KBr) 3294, 3051, 2937, 2835, 2231, 1695, 1601, 1545, 1510, 1454, 1415, 1352, 1304, 1236, 1169, 1134, 1080, 1005, 978, 843, 764, 714  $cm^{-1}$ ; <sup>1</sup>H NMR (600 MHz, CDCl<sub>3</sub>) δ 3.82 (3H, s), 3.86 (6H, s), 5.02 (2H, s), 6.71 (2H, s), 6.72 (1H, s), 8.01–8.22 (8H, m), 8.50 (1H, d, *J* = 8.4 Hz); <sup>13</sup>C NMR (150 MHz, CDCl<sub>3</sub>) δ 53.53, 56.12, 60.98, 71.80, 77.68, 78.29, 78.48, 96.54, 115.22, 124.01, 124.24, 124.42, 125.07, 125.98, 126.03, 126.42, 127.10, 128.91, 128.97, 130.64, 130.88, 131.08, 132.06, 133.44, 133.51, 134.38, 152.45 153.48. HRMS (ESI/Q-TOF) *m/z*: [M + Na]<sup>+</sup> calcd for C<sub>31</sub>H<sub>23</sub>NO<sub>5</sub>Na 512.1468; found 512.1486.

**5-(Pyren-1-yl)penta-2,4-diynyl N-(3,4,5-Trioctyloxyphenyl)carbamate (C<sub>8</sub>O-0).** A mixture of **4** (100 mg, 0.357 mmol), crude 3,4,5-trioctyloxyphenyl isocyanate (**9b**; 0.620 g), and a few drops of dibutyltin dilaurate in anhydrous THF (30 mL) was stirred overnight at ambient temperature. After the solvent in the reaction mixture was removed, the residue was purified by column chromatography (silica gel, chloroform) and recrystallized from a mixture of chloroform and methanol to afford **C<sub>8</sub>O-0** (230 mg, 0.293 mmol, 82%) as a pale orange powder: mp 106 °C; IR (KBr) 3303, 3041, 2954, 2924, 2852, 2231, 1697, 1601, 1540, 1508, 1468, 1433, 1379, 1348, 1300, 1240, 1176, 1132, 1080, 1020, 989, 847, 820, 760, 714  $cm^{-1}$ ; <sup>1</sup>H NMR (600 MHz, CDCl<sub>3</sub>) δ 0.85–0.91 (9H, m), 1.19–1.39 (24H, m), 1.44–1.50 (6H, m), 1.73 (2H, t, *J* = 7.2 Hz, 7.2 Hz), 1.79 (4H, t, *J* = 7.2 Hz, 7.2 Hz), 3.91 (2H, t, *J* = 7.2 Hz), 3.96 (6H, t, *J* = 7.2 Hz), 5.00 (2H, s), 6.64 (1H, s), 6.66 (2H, s), 8.02–8.25 (8H, m), 8.52 (1H, d, *J* = 9.0 Hz); <sup>13</sup>C NMR (150 MHz, CDCl<sub>3</sub>) δ 14.10, 22.66, 22.69, 26.06, 26.12, 29.28\*, 29.33\*, 29.36\*, 29.56\*, 30.28, 31.82, 31.90, 53.45, 69.11, 71.72, 73.52, 77.78, 78.32, 78.40, 97.83, 115.28, 124.03, 124.27, 124.44, 125.11, 125.98, 126.03, 126.43, 127.11, 128.91, 128.98, 130.66, 130.91, 131.10, 132.06, 132.84, 133.53, 134.51, 152.44, 153.33. Asterisks indicate overlapped peaks. Anal. Found: C, 79.71; H, 8.55; N, 1.75. Calcd for C<sub>52</sub>H<sub>65</sub>NO<sub>5</sub>: C, 79.66; H, 8.36; N, 1.79.

**5-(Pyren-6-yl)penta-2,4-diynyl N-(3,4,5-Tridodecyloxyphenyl)carbamate (C<sub>12</sub>O-0).** A mixture of **4** (200 mg, 0.713 mmol), crude 3,4,5-tridodecyloxyphenyl isocyanate (**9c**; 0.961 g), and a few drops of dibutyltin dilaurate in anhydrous THF (30 mL) was stirred overnight at ambient temperature. After the solvent in the reaction mixture was removed, the residue was purified by column chromatography (silica gel, chloroform) and recrystallized from a mixture of chloroform and methanol to afford **C<sub>12</sub>O-0** (470 mg, 0.493 mmol, 69%) as a pale orange powder: mp 104 °C; IR (KBr) 3288, 3045, 2917, 2850, 2231, 1693, 1601, 1539, 1465, 1431, 1382, 1346, 1298, 1230, 1178, 1120, 1080, 1020, 985, 843, 760, 715  $cm^{-1}$ ; <sup>1</sup>H NMR (400 MHz, CDCl<sub>3</sub>) δ 0.87 (9H, t, *J* = 6.8 Hz), 1.16–1.37 (48H, m), 1.43–1.48 (6H, m), 1.71–1.80 (6H, m), 3.91 (2H, t, *J* = 6.4 Hz), 3.95 (6H, t, *J* = 6.6 Hz), 5.00 (2H, s), 6.66 (2H, s), 6.68 (1H, br s), 7.99–8.22 (8H, m), 8.50 (1H, d, *J* = 9.2 Hz); <sup>13</sup>C NMR (100 MHz, CDCl<sub>3</sub>) δ 14.12, 22.68, 26.07, 26.12, 29.32\*, 29.36\*, 29.38\*, 29.40\*, 29.63\*, 29.69\*, 29.75\*, 30.27, 53.43, 69.05, 71.71, 73.49, 77.74, 78.30, 78.38, 97.74, 115.22, 123.98, 124.20, 124.40, 125.06, 125.93, 126.00, 126.38, 127.07, 128.87, 128.94, 130.60, 130.84, 131.04, 132.00, 132.85, 133.47, 134.40, 152.42, 153.30. Asterisks indicate overlapped peaks. Anal. Found: C, 80.50; H, 9.68; N, 1.41. Calcd for C<sub>64</sub>H<sub>89</sub>NO<sub>5</sub>: C, 80.71; H, 9.42; N, 1.47.

**5-(Pyren-1-yl)penta-2,4-diynyl N-(3,4,5-Trihexadecyloxyphenyl)carbamate (C<sub>16</sub>O-0).** A mixture of **4** (100 mg, 0.357 mmol), crude 3,4,5-trihexadecyloxyphenyl isocyanate (**9d**; 1.19 g), and a few drops of dibutyltin dilaurate in anhydrous THF (20 mL) was stirred overnight at ambient temperature. After the

solvent in the reaction mixture was removed, the residue was purified by column chromatography (silica gel, chloroform) and recrystallized from a mixture of chloroform and methanol to afford **C<sub>16</sub>O-0** (100 mg, 0.0892 mmol, 25%) as a pale orange solid: mp 109 °C; IR (KBr) 3290, 3045, 2916, 2848, 2231, 1693, 1599, 1537, 1466, 1431, 1383, 1344, 1298, 1227, 1120, 1081, 1016, 987, 843, 765, 715  $cm^{-1}$ ; <sup>1</sup>H NMR (600 MHz, CDCl<sub>3</sub>) δ 0.85–0.90 (9H, m), 1.21–1.36 (72H, m), 1.42–1.50 (6H, m), 1.72–1.82 (6H, m), 3.91 (2H, t, *J* = 6.5 Hz), 3.97 (6H, t, *J* = 6.5 Hz), 5.00 (2H, s), 6.61 (1H, s), 6.66 (2H, s), 8.03–8.26 (8H, m), 8.53 (1H, d, *J* = 9.0 Hz); <sup>13</sup>C NMR (150 MHz, CDCl<sub>3</sub>) δ 14.11, 22.68, 26.08, 26.14, 29.37\*, 29.42\*, 29.64\*, 29.71\*, 29.75\*, 30.29, 31.92, 53.46, 69.14, 71.73, 73.52, 77.77, 78.33, 78.41, 97.84, 115.31, 124.06, 124.30, 124.45, 125.13, 125.99, 126.05, 126.44, 127.13, 128.92, 128.99, 130.67, 130.93, 131.13, 132.07, 132.83, 133.55, 134.57, 152.37, 153.34. Asterisks indicate overlapped peaks. Anal. Found: C, 81.44; H, 10.20; N, 1.23. Calcd for C<sub>76</sub>H<sub>113</sub>NO<sub>5</sub>: C, 81.45; H, 10.16; N, 1.25.

**5-(Pyren-1-yl)penta-2,4-diynyl N-[(3,4,5-Trimethoxyphenyl)methyl]carbamate (C<sub>1</sub>O-1).** A mixture of **4** (0.100 g, 0.357 mmol), crude (3,4,5-trimethoxyphenyl)methyl isocyanate (**15a**; 0.440 g), and a few drops of dibutyltin dilaurate in anhydrous THF (30 mL) was stirred overnight at ambient temperature. After the solvent in the reaction mixture was removed, the residue was purified by column chromatography (silica gel, chloroform/ethyl acetate 9/1) and recrystallized from a mixture of chloroform and methanol to afford **C<sub>1</sub>O-1** (100 mg, 0.199 mmol, 56%) as an orange powder: mp 164 °C; IR (KBr) 3311, 3047, 2925, 2231, 1722, 1597, 1508, 1464, 1423, 1377, 1329, 1244, 1126, 1038, 993, 845, 777, 715  $cm^{-1}$ ; <sup>1</sup>H NMR (600 MHz, CDCl<sub>3</sub>) δ 3.83 (3H, s), 3.87 (6H, s), 4.36 (2H, d, *J* = 6.0 Hz), 4.97 (2H, s), 5.23 (1H, s), 6.54 (2H, s), 8.01–8.23 (8H, m), 8.50 (1H, d, *J* = 9.0 Hz); <sup>13</sup>C NMR (150 MHz, CDCl<sub>3</sub>) δ 45.55, 53.41, 56.13, 60.81, 71.38, 78.21, 78.35, 104.49, 115.27, 124.01, 124.25, 124.41, 125.04, 125.95, 126.00, 126.40, 127.09, 128.88, 128.95, 130.60, 130.88, 131.08, 132.03, 133.47, 133.77, 137.38, 153.44, 155.44. HRMS (ESI/Q-TOF) *m/z*: [M + Na]<sup>+</sup> calcd for C<sub>32</sub>H<sub>25</sub>NO<sub>5</sub>Na 526.1625; found 526.1631.

**5-(Pyren-1-yl)penta-2,4-diynyl N-[(3,4,5-Trioctyloxyphenyl)methyl]carbamate (C<sub>8</sub>O-1).** A mixture of **4** (80.0 mg, 0.285 mmol), crude (3,4,5-trioctyloxyphenyl)methyl isocyanate (**15b**; 0.270 g), and a few drops of dibutyltin dilaurate in anhydrous THF (30 mL) was stirred overnight at ambient temperature. After the solvent in the reaction mixture was removed, the residue was purified by column chromatography (silica gel, chloroform/ethyl acetate 9/1) and recrystallized from a mixture of chloroform and methanol to afford **C<sub>8</sub>O-1** (120 mg, 0.150 mmol, 53%) as a yellowish green solid: mp 105 °C; IR (KBr) 3307, 3043, 2921, 2280, 2235, 1693, 1592, 1552, 1508, 1442, 1383, 1331, 1277, 1228, 1119, 1054, 978, 845, 754, 715  $cm^{-1}$ ; <sup>1</sup>H NMR (600 MHz, CDCl<sub>3</sub>) δ 0.83–0.89 (9H, m), 1.17–1.35 (24H, m), 1.40–1.49 (6H, m), 1.69–1.81 (6H, m), 3.92 (2H, t, *J* = 6.6 Hz), 3.96 (4H, t, *J* = 6.6 Hz), 4.32 (2H, d, *J* = 6.0 Hz), 4.96 (2H, s), 5.14 (1H, t, *J* = 6.0 Hz), 6.49 (2H, s), 8.00–8.24 (8H, m), 8.50 (1H, d, *J* = 8.4 Hz); <sup>13</sup>C NMR (150 MHz, CDCl<sub>3</sub>) δ 14.07, 22.63, 22.66, 26.08, 29.26\*, 29.35\*, 29.53\*, 30.29, 31.79, 31.87, 45.60, 53.37, 69.11, 71.36, 73.41, 78.16, 78.25, 78.38, 105.92, 115.31, 124.00, 124.23, 124.41, 125.08, 125.93, 125.99, 126.39, 127.09, 128.86, 128.93, 130.61, 130.88, 131.07, 132.00, 133.02, 133.47, 137.52, 153.32, 155.37. Asterisks indicate overlapped peaks. Anal. Found: C, 79.48; H, 8.70; N, 1.75. Calcd for C<sub>53</sub>H<sub>67</sub>NO<sub>5</sub>: C, 79.76; H, 8.46; N, 1.75.

**5-(Pyren-1-yl)penta-2,4-diynyl N-[(3,4,5-Tridodecyloxyphenyl)methyl]carbamate (C<sub>12</sub>O-1).** A mixture of **4** (300 mg, 1.07 mmol), crude (3,4,5-tridodecyloxyphenyl)methyl isocyanate (**15c**; 1.36 g), and a few drops of dibutyltin dilaurate in anhydrous THF (30 mL) was stirred overnight at ambient temperature. After the solvent in the reaction mixture was removed, the residue was purified by column chromatography (silica gel, chloroform/ethyl acetate 9/1) and recrystallized from a mixture of chloroform and methanol to afford **C<sub>12</sub>O-1** (540 mg, 0.559 mmol, 52%) as a yellowish green solid: mp 97 °C; IR (KBr) 3309, 3009, 2920, 2850, 2237, 1693, 1593, 1552, 1508, 1468, 1439, 1387, 1331,

1265, 1220, 1055, 973, 843, 714  $\text{cm}^{-1}$ ;  $^1\text{H}$  NMR (600 MHz,  $\text{CDCl}_3$ )  $\delta$  0.85–0.89 (9H, m), 1.16–1.34 (48H, m), 1.41–1.48 (6H, m), 1.69–1.81 (6H, m), 3.92 (2H, t,  $J = 6.6$  Hz), 3.97 (4H, t,  $J = 6.6$  Hz), 4.32 (2H, d,  $J = 5.7$  Hz), 4.96 (2H, s), 5.12 (1H, t,  $J = 5.7$  Hz), 6.49 (2H, s), 8.02–8.25 (8H, m), 8.52 (1H, d,  $J = 9.0$  Hz);  $^{13}\text{C}$  NMR (150 MHz,  $\text{CDCl}_3$ )  $\delta$  14.10, 22.67, 26.10, 29.35\*, 29.38\*, 29.41\*, 29.62\*, 29.67\*, 29.74\*, 30.31, 31.90, 45.61, 53.38, 69.15, 71.37, 73.42, 78.18, 78.25, 78.41, 105.97, 115.36, 124.05, 124.28, 124.43, 125.12, 125.96, 126.02, 126.41, 127.11, 128.89, 128.96, 130.64, 130.92, 131.12, 132.04, 133.02, 133.52, 137.60, 153.35, 155.37. Asterisks indicate overlapped peaks. Anal. Found: C, 80.59; H, 9.55; N, 1.36. Calcd for  $\text{C}_{63}\text{H}_{91}\text{NO}_5$ : C, 80.78; H, 9.49; N, 1.45.

**5-(Pyren-1-yl)penta-2,4-diynyl N-[(3,4,5-Trihexadecyloxyphenyl)methyl]carbamate ( $\text{C}_{16}\text{O}-1$ ).** A mixture of **4** (80.0 mg, 0.285 mmol), crude (3,4,5-trihexadecyloxyphenyl)-methyl isocyanate (**15d**; 0.500 g), and a few drops of dibutyltin dilaurate in anhydrous THF (30 mL) was stirred overnight at ambient temperature. After the solvent in the reaction mixture was removed, the residue was purified by column chromatography (silica gel, chloroform/ethyl acetate 9/1) and recrystallized from a mixture of chloroform and methanol to afford  $\text{C}_{16}\text{O}-1$  (80.0 mg, 0.0705 mmol, 25%) as a yellowish green solid: mp 78  $^\circ\text{C}$ ; IR (KBr) 3307, 3043, 2918, 2848, 2237, 1693, 1592, 1554, 1508, 1468, 1439, 1385, 1331, 1267, 1230, 1122, 1055, 968, 842, 715  $\text{cm}^{-1}$ ;  $^1\text{H}$  NMR (600 MHz,  $\text{CDCl}_3$ )  $\delta$  0.87 (9H, t,  $J = 6.9$  Hz), 1.17–1.34 (72H, m), 1.40–1.48 (6H, m), 1.69–1.81 (6H, m), 3.92 (2H, t,  $J = 6.6$  Hz), 3.97 (4H, t,  $J = 6.6$  Hz), 4.32 (2H, d,  $J = 5.6$  Hz), 4.96 (2H, s), 5.11 (1H, t,  $J = 5.6$  Hz), 6.49 (2H, s), 8.02–8.25 (8H, m), 8.53 (1H, d,  $J = 9.0$  Hz);  $^{13}\text{C}$  NMR (150 MHz,  $\text{CDCl}_3$ )  $\delta$  14.10, 22.68, 26.11, 29.36\*, 29.42\*, 29.63\*, 29.65\*, 29.70\*, 29.74\*, 30.31, 31.91, 45.61, 53.38, 69.15, 71.37, 73.42, 78.18, 78.25, 78.40, 105.95, 115.36, 124.05, 124.28, 124.43, 125.12, 125.96, 126.02, 126.42, 127.11, 128.89, 128.96, 130.65, 130.92, 131.12, 132.04, 133.03, 133.52, 137.58, 153.34, 155.37. Asterisks indicate overlapped peaks. Anal. Found: C, 81.20; H, 10.89; N, 1.41%. Calcd for  $\text{C}_{77}\text{H}_{115}\text{NO}_5$ : C, 81.50; H, 10.21; N, 1.23.

**Characterization Methods and Apparatus.** UV–vis diffuse reflectance and absorption spectra were measured using a Jasco V-570 spectrophotometer, and an integrated sphere (ILN-472) was attached to obtain the diffuse reflectance spectra. The samples for the diffuse reflectance spectra were prepared by grinding solid compounds with potassium bromide, and the mixtures were placed in a sample cell with a quartz window for the measurements. FT-IR spectra were recorded on a Horiba FT-720 spectrometer. Melting points were measured using a SII TG/DTA 6200 calorimeter.  $^1\text{H}$  and  $^{13}\text{C}$  NMR spectra were measured using a JEOL ECX-400 or ECZ-600 spectrometer. Elemental analyses were performed on a PerkinElmer CHN/O 2400 II analyzer. High-resolution electrospray ionization time-of-flight mass spectrometry (ESI-TOF-MS) was obtained by using a Bruker micrOTOF-Q II mass spectrometer in the positive ion mode.

Powder X-ray diffraction patterns were measured using a synchrotron radiation X-ray beam with a wavelength of 1.00  $\text{\AA}$  at the BL40B2 beamline at SPring-8 (Hyogo, Japan). Single crystals of  $\text{C}_1\text{O}-0$  and  $\text{C}_1\text{O}-1$  were obtained by the slow evaporation of a solution of a chloroform/methanol (1/1) mixture. X-ray crystallographic analyses of  $\text{C}_1\text{O}-0$  and  $\text{C}_1\text{O}-1$  were performed at the beamlines of BL40XU with an X-ray wavelength of 0.78192  $\text{\AA}$  and BL02B1 with that of 0.4249  $\text{\AA}$ , respectively, at SPring-8 (Hyogo, Japan). The structures were solved by direct methods. All non-hydrogen atoms were refined anisotropically.

Photopolymerization was performed by UV irradiation at 254 nm using a 4 W lamp (UVP, UVG-11). GPC was performed using two serially connected Tosoh TSKgel G4000H<sub>HR</sub> columns with a Jasco PU-980 pump and a UV-975 UV–vis detector. The eluent was chloroform, and polystyrene was used as a molecular weight standard. The electrical conductivity was evaluated for the cast films at room temperature from  $I$ – $V$  curves measured using an apparatus based on a Keithley 2400 SourceMeter. On glass slides, gold electrodes with an electrode gap of 50  $\mu\text{m}$  were prepared using VPC-060 vacuum

deposition equipment (ULVAC Kiko), and chloroform solutions of the compounds were cast on the slides to form the films. The film thickness was measured using a Surfcoater ET200 microfigure measuring instrument (Kosaka Laboratory).

## ■ ASSOCIATED CONTENT

### Supporting Information

The Supporting Information is available free of charge at <https://pubs.acs.org/doi/10.1021/acs.cgd.0c00438>.

Fluorescence spectra and synthesis of phenyl and benzyl isocyanates (PDF)

### Accession Codes

CCDC 1993204–1993205 contain the supplementary crystallographic data for this paper. These data can be obtained free of charge via [www.ccdc.cam.ac.uk/data\\_request/cif](http://www.ccdc.cam.ac.uk/data_request/cif), or by emailing [data\\_request@ccdc.cam.ac.uk](mailto:data_request@ccdc.cam.ac.uk), or by contacting The Cambridge Crystallographic Data Centre, 12 Union Road, Cambridge CB2 1EZ, UK; fax: +44 1223 336033.

## ■ AUTHOR INFORMATION

### Corresponding Author

Shuji Okada – Graduate School of Organic Materials Science and Faculty of Engineering, Yamagata University, Yonezawa 992-8510, Japan; [orcid.org/0000-0001-9519-6648](https://orcid.org/0000-0001-9519-6648); Email: [okadas@yz.yamagata-u.ac.jp](mailto:okadas@yz.yamagata-u.ac.jp)

### Authors

Shuhei Oshimizu – Graduate School of Organic Materials Science, Yamagata University, Yonezawa 992-8510, Japan  
Shoko Takeshi – Faculty of Engineering, Yamagata University, Yonezawa 992-8510, Japan  
Tsubasa Sato – Faculty of Engineering, Yamagata University, Yonezawa 992-8510, Japan  
Ryohei Yamakado – Graduate School of Organic Materials Science and Faculty of Engineering, Yamagata University, Yonezawa 992-8510, Japan; [orcid.org/0000-0003-4085-9226](https://orcid.org/0000-0003-4085-9226)  
Yoko Tatewaki – Division of Applied Chemistry, Tokyo University of Agriculture and Technology, Koganei 184-8588, Japan

Complete contact information is available at: <https://pubs.acs.org/doi/10.1021/acs.cgd.0c00438>

### Notes

The authors declare no competing financial interest.

## ■ ACKNOWLEDGMENTS

The synchrotron radiation experiments were performed at the BL40B2 (2017B1294), BL02B1 (2018B1714) and BL40XU (2019A1211) of SPring-8 with the approval of the Japan Synchrotron Radiation Research Institute (JASRI) with the supports by Dr. Noboru Ohta, JASRI/SPring-8, Dr. Kunihisa Sugimoto, JASRI/SPring-8, and Dr. Nobuhiro Yasuda, JASRI/SPring-8.

## ■ REFERENCES

- (1) Sauteret, C.; Hermann, J.-P.; Frey, R.; Pradère, F.; Ducuing, J.; Baughman, R. H.; Chance, R. R. Optical Nonlinearities in One-Dimensional-Conjugated Polymer Crystals. *Phys. Rev. Lett.* **1976**, *36*, 956–959.
- (2) Yamamoto, T.; Yamada, W.; Takagi, M.; Kizu, K.; Maruyama, T.; Ooba, N.; Tomaru, S.; Kurihara, T.; Kaino, T.; Kubota, K. P-Conjugated Soluble Poly(aryleneethynylene) Type Polymers. Prep-

- aration by Palladium-Catalyzed Coupling Reaction, Nonlinear Optical Properties, Doping, and Chemical Reactivity. *Macromolecules* **1994**, *27*, 6620–6626.
- (3) Hegde, P. K.; Adhikari, A. V.; Manjunatha, M. G.; Poornesh, P.; Umesh, G. Third-Order Nonlinear Optical Susceptibilities of New Copolymers Containing Alternate 3,4-Dialkoxythiophene and (1,3,4-Oxadiazolyl)pyridine Moieties. *Opt. Mater.* **2009**, *31*, 1000–1006.
- (4) Shirakawa, H.; Louis, E. J.; MacDiarmid, A. G.; Chiang, C. K.; Heeger, A. J. Synthesis of Electrically Conducting Organic Polymers: Halogen Derivatives of Polyacetylene,  $(\text{CH})_x$ . *J. Chem. Soc., Chem. Commun.* **1977**, 578–580.
- (5) Pron, A.; Rannou, P. Processible Conjugated Polymers: From Organic Semiconductors to Organic Metals and Superconductors. *Prog. Polym. Sci.* **2002**, *27*, 135–190.
- (6) Osaka, I.; McCullough, R. D. Advances in Molecular Design and Synthesis of Regioregular Polythiophenes. *Acc. Chem. Res.* **2008**, *41*, 1202–1214.
- (7) Kobayashi, T.; Yoneyama, H.; Tamura, H. Electrochemical Reactions Concerned with Electrochromism of Polyaniline Film-Coated Electrodes. *J. Electroanal. Chem. Interfacial Electrochem.* **1984**, *177*, 281–291.
- (8) Argun, A. A.; Aubert, P.-H.; Thompson, B. C.; Schwendeman, L.; Gaupp, C. L.; Hwang, J.; Pinto, N. J.; Tanner, D. B.; MacDiarmid, A. G.; Reynolds, J. R. Multicolored Electrochromism in Polymers: Structures and Devices. *Chem. Mater.* **2004**, *16*, 4401–4412.
- (9) Savagian, L. R.; Österholm, A. M.; Shen, D. E.; Christiansen, D. T.; Kuempfert, M.; Reynolds, J. R. Conjugated Polymer Blends for High Contrast Black-to-Transmissive Electrochromism. *Adv. Opt. Mater.* **2018**, *6*, 1800594.
- (10) Burroughes, J. H.; Bradley, D. D. C.; Brown, A. R.; Marks, R. N.; Mackay, K.; Friend, R. H.; Burns, P. L.; Holmes, A. B. Light-Emitting Diodes Based on Conjugated Polymers. *Nature* **1990**, *347*, 539–541.
- (11) Kraft, A.; Grimsdale, A. C.; Holmes, A. B. Electroluminescent Conjugated Polymers—Seeing Polymers in a New Light. *Angew. Chem., Int. Ed.* **1998**, *37*, 402–428.
- (12) Zhang, X.; Kale, D. M.; Jenekhe, S. A. Electroluminescence of Multicomponent Conjugated Polymers. 2. Photophysics and Enhancement of Electroluminescence from Blends of Polyquinolines. *Macromolecules* **2002**, *35*, 382–393.
- (13) Sariciftci, N. S.; Braun, D.; Zhang, C.; Srdanov, V. I.; Heeger, A. J.; Stucky, G.; Wudl, F. Semiconducting Polymer-Buckminsterfullerene Heterojunctions: Diodes, Photodiodes, and Photovoltaic Cells. *Appl. Phys. Lett.* **1993**, *62*, 585–587.
- (14) Günes, S.; Neugebauer, H.; Sariciftci, N. S. Conjugated Polymer-Based Organic Solar Cells. *Chem. Rev.* **2007**, *107*, 1324–1338.
- (15) Facchetti, A.  $\pi$ -Conjugated Polymers for Organic Electronics and Photovoltaic Cell Applications. *Chem. Mater.* **2011**, *23*, 733–758.
- (16) Adegoke, O. O.; Jung, I. H.; Orr, M.; Yu, L.; Goodson, T., III Effect of Acceptor Strength on Optical and Electronic Properties in Conjugated Polymers for Solar Applications. *J. Am. Chem. Soc.* **2015**, *137*, 5759–5769.
- (17) Fuchigami, H.; Tsumura, A.; Koezuka, H. Polythiophenevinylene Thin-Film Transistor with High Carrier Mobility. *Appl. Phys. Lett.* **1993**, *63*, 1372–1374.
- (18) Hamilton, M. C.; Kanicki, J. Organic Polymer Thin-Film Transistor Photosensors. *IEEE J. Sel. Top. Quantum Electron.* **2004**, *10*, 840–848.
- (19) Lee, J.; Han, A.-R.; Kim, J.; Kim, Y.; Oh, J. H.; Yang, C. Solution-Processable Ambipolar Diketopyrrolopyrrole-Selenophene Polymer with Unprecedentedly High Hole and Electron Mobilities. *J. Am. Chem. Soc.* **2012**, *134*, 20713–20721.
- (20) McQuade, D. T.; Pullen, A. E.; Swager, T. M. Conjugated Polymer-Based Chemical Sensors. *Chem. Rev.* **2000**, *100*, 2537–2574.
- (21) Janata, J.; Josowicz, M. Conducting Polymers in Electronic Chemical Sensors. *Nat. Mater.* **2003**, *2*, 19–24.
- (22) Le Maout, P.; Wojkiewicz, J.-L.; Redon, N.; Lahuec, C.; Seguin, F.; Dupont, L.; Mikhaylov, S.; Noskov, Y.; Ogurtsov, N.; Pud, A. Polyaniline Nanocomposites Based Sensor Array for Breath Ammonia Analysis. Portable E-nose Approach to Non-invasive Diagnosis of Chronic Kidney Disease. *Sens. Actuators, B* **2018**, *274*, 616–626.
- (23) Wegner, G. Topochemische Reaktionen von Monomeren mit konjugierten Dreifachbindungen I. Mitt.: Polymerisation von Derivaten des 2,4-Hexadiin-1,6-diols im kristallinen Zustand. *Z. Naturforsch., B: J. Chem. Sci.* **1969**, *24B*, 824–832.
- (24) Baughman, R. H.; Yee, K. C. Solid-State Polymerization of Linear and Cyclic Acetylenes. *Macromol. Rev.* **1978**, *13*, 219–239.
- (25) Enkelmann, V. Structural Aspects of the Topochemical Polymerization of Diacetylenes. In *Polydiacetylenes: Adv. Polym. Sci.*; Cantow, H.-J., Ed.; Springer-Verlag: Berlin, 1984; Vol. 63, pp 91–136.
- (26) Carter, G. M.; Hryniewicz, J. V.; Thakur, M. K.; Chen, Y. J.; Meyler, S. E. Nonlinear Optical Processes in a Polydiacetylene Measured with Femtosecond Duration Laser Pulses. *Appl. Phys. Lett.* **1986**, *49*, 998–1000.
- (27) Hattori, T.; Kobayashi, T. Femtosecond Dephasing in a Polydiacetylene Film Measured by Degenerate Four-Wave Mixing with an Incoherent Nanosecond Laser. *Chem. Phys. Lett.* **1987**, *133*, 230–234.
- (28) Kanetake, T.; Ishikawa, K.; Hasegawa, T.; Koda, T. Nonlinear Optical Properties of Highly Oriented Polydiacetylene Evaporated Films. *Appl. Phys. Lett.* **1989**, *54*, 2287–2289.
- (29) Okada, S.; Ohsugi, M.; Masaki, A.; Matsuda, H.; Takaragi, S.; Nakanishi, H. Preparation and Nonlinear Optical Property of Polydiacetylenes from Unsymmetrical Diphenylbutadiynes with Trifluoromethyl Substituents. *Mol. Cryst. Liq. Cryst.* **1990**, *183*, 81–90.
- (30) Rochford, K.; Zanon, R.; Stegeman, G. I. Measurement of Nonlinear Refractive Index and Transmission in Polydiacetylene Waveguides at 1.319  $\mu\text{m}$ . *Appl. Phys. Lett.* **1991**, *58*, 13–15.
- (31) Bakarezos, M.; Camacho, M. A.; Blewett, I. J.; Kar, A. K.; Wherrett, B. S.; Matsuda, H.; Fukuda, T.; Yamada, S.; Rangel-Rojo, R.; Katagi, H.; Kasai, H.; Okada, S.; Nakanishi, H. Ultrafast Nonlinear Refraction in Integrated Fabry-Perot Etalon Containing Polydiacetylene. *Electron. Lett.* **1999**, *35*, 1078–1079.
- (32) Se, K.; Ohnuma, H.; Kotaka, T. Electrical Conductivity of Urethane-Substituted Poly(diacetylenes): Effect of Substituent Side Groups and Molecular Weights. *Macromolecules* **1984**, *17* (10), 2126–2131.
- (33) Nakanishi, H.; Matsuda, H.; Kato, M. Preparation of a Variety of Polymeric Conductors from Diacetylenes. *Mol. Cryst. Liq. Cryst.* **1984**, *105*, 77–88.
- (34) Marikhin, V. A.; Guk, E. G.; Myasnikova, L. P. New Approach to Achieving the Potentially High Conductivity of Polydiacetylene. *Phys. Solid State* **1997**, *39*, 686–689.
- (35) Matsuda, H.; Nakanishi, H.; Kato, S.; Kato, M. Conductivity of Polydiacetylene with  $\pi$ -Conjugation between Polymer Backbone and Substituents. *J. Polym. Sci., Part A: Polym. Chem.* **1987**, *25*, 1663–1669.
- (36) Shimada, S.; Masaki, A.; Matsuda, H.; Okada, S.; Nakanishi, H. Molecular Architecture of Regularly Mixed  $\pi$ -Conjugated Systems Using Diacetylene Solid-State Polymerization. *Mol. Cryst. Liq. Cryst. Sci. Technol., Sect. A* **1998**, *315*, 83–92.
- (37) Takami, K.; Kuwahara, Y.; Ishii, T.; Akai-Kasaya, M.; Saito, A.; Aono, M. Significant Increase in Conductivity of Polydiacetylene Thin Film Induced by Iodine Doping. *Surf. Sci.* **2005**, *591*, L273–L279.
- (38) Okada, S.; Peng, S.; Spevak, W.; Charych, D. Color and Chromism of Polydiacetylene Vesicles. *Acc. Chem. Res.* **1998**, *31*, 229–239.
- (39) Reppy, M. A.; Pindzola, B. A. Biosensing with Polydiacetylene Materials: Structures, Optical Properties and Applications. *Chem. Commun.* **2007**, *42*, 4317–4338.
- (40) Ahn, D. J.; Kim, J.-M. Fluorogenic Polydiacetylene Supramolecules: Immobilization, Micropatterning, and Application to Label-Free Chemosensors. *Acc. Chem. Res.* **2008**, *41*, 805–816.
- (41) Jelinek, R.; Ritenberg, M. Polydiacetylene—Recent Molecular Advances and Applications. *RSC Adv.* **2013**, *3*, 21192–21201.

- (42) Orchard, B. J.; Tripathy, S. K. Molecular Structure and Electronic Property Modification of Poly(diacetylenes). *Macromolecules* **1986**, *19*, 1844–1850.
- (43) Curtis, S. M.; Le, N.; Fowler, F. W.; Lauher, J. W. A Rational Approach to the Preparation of Polydipyridyldiacetylenes: An Exercise in Crystal Design. *Cryst. Growth Des.* **2005**, *5*, 2313–2321.
- (44) Lauher, J. W.; Fowler, F. W.; Goroff, N. S. Single-Crystal-to-Single-Crystal Topochemical Polymerizations by Design. *Acc. Chem. Res.* **2008**, *41*, 1215–1229.
- (45) Nakanishi, H.; Matsuda, H.; Okada, S.; Kato, M. Preparation and Nonlinear Optical Properties of Novel Polydiacetylenes. In *Frontiers of Macromolecular Science*; Saegusa, T., Higashimura, T., Abe, A., Eds.; Blackwell Scientific: Oxford, 1989; pp 469–474.
- (46) Sarkar, A.; Okada, S.; Matsuzawa, H.; Matsuda, H.; Nakanishi, H. Novel Polydiacetylenes for Optical Materials: Beyond the Conventional Polydiacetylenes. *J. Mater. Chem.* **2000**, *10*, 819–828.
- (47) Tatewaki, Y.; Shibata, H.; Shibuya, T.; Watanabe, K.; Ishii, S.; Okada, S. Solid-State Polymerization of a Pyrenylbutadiyne Derivative. In *Polymer Photonics and Novel Optical Technologies*; Kawabe, Y., Kawase, M., Eds.; Photonics World Consortium: Chitose, 2011; pp 152–155.
- (48) Tatewaki, Y.; Sato, A.; Ito, S.; Inayama, S.; Okada, S. Synthesis and Solid-State Polymerization of L-Alanine Derivatives with a (1-Pyrenyl)butadiynyl Group. *Mol. Cryst. Liq. Cryst.* **2013**, *580*, 58–63.
- (49) Ikeshima, M.; Mamada, M.; Katagiri, H.; Minami, T.; Okada, S.; Tokito, S. Synthesis and Solid-State Polymerization of Diacetylene Derivatives with an N-Carbazolylphenyl Group. *Bull. Chem. Soc. Jpn.* **2015**, *88*, 843–849.
- (50) Ikeshima, M.; Mamada, M.; Minami, T.; Tokito, S.; Okada, S. Synthesis and Solid-State Polymerization of Diacetylene Derivatives Directly Substituted by a Phenylcarbazole Moiety. *Polym. J.* **2016**, *48*, 1013–1018.
- (51) Ishii, S.; Kaneko, S.; Tatewaki, Y.; Okada, S. Synthesis and Solid-State Polymerization of 4-(Dimethylamino)phenylbutadiyne Derivatives and Their Charge-Transfer Complexes. *Mol. Cryst. Liq. Cryst.* **2013**, *580*, 64–68.
- (52) Ikeshima, M.; Katagiri, H.; Fujiwara, W.; Tokito, S.; Okada, S. Synthesis, Crystal Structures and Solid-State Polymerization of 8-[4-(Dimethylamino)phenyl]octa-5,7-diyne Carbamates. *Cryst. Growth Des.* **2018**, *18*, 5991–6000.
- (53) Imai, M.; Tatewaki, Y.; Okada, S. Preparation and Physical Properties of Nanoaggregates Composed of Charge-Transfer Complexes Containing Butadiyne Derivatives with Tetrathiafulvalene Moieties. *Jpn. J. Appl. Phys.* **2014**, *53*, 05FA02.
- (54) Patel, G. N.; Chance, R. R.; Witt, J. D. A Visual Conformational Transition in a Polymer Solution. *J. Polym. Sci., Polym. Lett. Ed.* **1978**, *16*, 607–614.
- (55) Sukwattanasinitt, M.; Lee, D.-C.; Kim, M.; Wang, X.; Li, L.; Yang, K.; Kumar, J.; Tripathy, S. K.; Sandman, D. J. New Processable, Functionalizable Polydiacetylenes. *Macromolecules* **1999**, *32*, 7361–7369.
- (56) Takahashi, R.; Nunokawa, T.; Shibuya, T.; Tomita, R.; Tatewaki, Y.; Okada, S.; Kimura, T.; Shimada, S.; Matsuda, H. Synthesis and Solid-State Polymerization of Butadiyne Derivatives with Trialkoxyphenylurethane Groups. *Bull. Chem. Soc. Jpn.* **2012**, *85*, 236–244.
- (57) Kikuchi, K.; Tatewaki, Y.; Okada, S. Self-Assembly and Solid-State Polymerization of Butadiyne Derivatives with Amide and Trialkoxyphenyl Groups. *Bull. Chem. Soc. Jpn.* **2017**, *90*, 298–305.
- (58) Rubner, M. F. Synthesis and Characterization of Polyurethane-Diacetylene Segmented Copolymers. *Macromolecules* **1986**, *19*, 2114–2128.
- (59) Beckham, H. W.; Rubner, M. F. Synthesis and Optical Properties of a New Class of Polyamides Containing Reactive Diacetylene Groups. *Macromolecules* **1989**, *22*, 2130–2138.
- (60) Beckham, H. W.; Rubner, M. F. Structural Characterization of the Cross-Polymerization of a Diacetylene-Functionalized Polyamide. *Macromolecules* **1993**, *26*, 5192–5197.
- (61) Day, D. R.; Lando, J. B. Conduction in Polydiacetylene Bilayers. *J. Appl. Polym. Sci.* **1981**, *26*, 1605–1612.
- (62) Se, K.; Ohnuma, H.; Kotaka, T. Urethane-Substituted Polydiacetylenes: Structure and Electrical Properties of Poly[4,6-decadiyne-1,10-diol bis[(n-butoxycarbonyl)methyl]urethane]. *Macromolecules* **1983**, *16*, 1581–1587.
- (63) Tanaka, Y.; Matsuda, H.; Iijima, S.; Fujikawa, H.; Nakanishi, H.; Kato, M.; Kato, S. High Pressure Solid State Polymerization of 1,4-Bis(p-toluenesulfonyloxymethyl)-1,3-butadiyne. *Makromol. Chem., Rapid Commun.* **1985**, *6*, 715–720.
- (64) Qian, R.; Shi, S.; Liu, T.; Zhu, D. Carrier Transport Properties of Poly(1,6-bis-9-carbazolyl-2,4-hexadiyne). *Phys. Status Solidi A* **1989**, *111*, K67–K71.
- (65) Takami, K.; Mizuno, J.; Akai-Kasaya, M.; Saito, A.; Aono, M.; Kuwahara, Y. Conductivity Measurement of Polydiacetylene Thin Films by Double-Tip Scanning Tunneling Microscopy. *J. Phys. Chem. B* **2004**, *108*, 16353–16356.
- (66) Jiang, H.; Hershtig, G.; Richter, S.; Jelinek, R. Light-Induced Conductivity in a Solution-Processed Film of Polydiacetylene and Perylene Diimide. *J. Phys. Chem. Lett.* **2016**, *7*, 1628–1631.
- (67) Tang, Z.; Li, M.; Song, M.; Jiang, L.; Li, J.; He, Y.; Zhou, L. Good Conductivity of a Single Component Polydiacetylene Film. *Org. Electron.* **2017**, *49*, 174–178.
- (68) Melby, L. R.; Harder, R. J.; Hertler, W. R.; Mahler, W.; Benson, R. E.; Mochel, W. E. Substituted Quinodimethans. II. Anion-radical Derivatives and Complexes of 7,7,8,8-Tetracyanoquinodimethane. *J. Am. Chem. Soc.* **1962**, *84*, 3374–3387.
- (69) Prout, C. K.; Tickle, I. J.; Wright, J. D. Molecular Complexes. XVI. Crystal Structure of the 1:1 Molecular Complex of Pyrene and 7,7,8,8-Tetracyanoquinodimethane. *J. Chem. Soc., Perkin Trans. 2* **1973**, 528–530.
- (70) Emge, T. J.; Maxfield, M.; Cowan, D. O.; Kistenmacher, T. J. Solution and Solid State Studies of Tetrafluoro-7,7,8,8-Tetracyano-p-Quinodimethane, TCNQF<sub>4</sub>. Evidence for Long-Range Amphoteric Intermolecular Interactions and Low-Dimensionality in the Solid State Structure. *Mol. Cryst. Liq. Cryst.* **1981**, *65*, 161–178.
- (71) Schofield, E.; Schulz, R. C. Synthesis and Complex Formation of 1,6-Bis(3-pyrenyloxy)-2,4-hexadiyne. *Makromol. Chem., Rapid Commun.* **1981**, *2*, 677–681.
- (72) Dobrowolski, M. A.; Garbarino, G.; Mezouar, M.; Ciesielski, A.; Cyranski, M. K. Structural Diversities of Charge Transfer Organic Complexes. Focus on Benzenoid Hydrocarbons and 7,7,8,8-Tetracyanoquinodimethane. *CrystEngComm* **2014**, *16*, 415–429.
- (73) Sun, H.; Wang, M.; Wei, X.; Zhang, R.; Wang, S.; Khan, A.; Usman, R.; Feng, Q.; Du, M.; Yu, F.; Zhang, W.; Xu, C. Understanding Charge-Transfer Interaction Mode in Cocrystals and Solvates of 1-Phenyl-3-(pyren-1-yl)prop-2-en-1-one and TCNQ. *Cryst. Growth Des.* **2015**, *15*, 4032–4038.
- (74) Tanaka, Y.; Iijima, S.; Shimizu, T.; Fujikawa, H.; Matsuda, H.; Nakanishi, H.; Kato, M.; Kato, S. Solid-state Polymerization of 1,4-Bis(3-acetylaminophenyl)-1,3-butadiyne under High Pressure. *J. Polym. Sci., Part C: Polym. Lett.* **1986**, *24*, 177–184.